

# Demonstration of the coupling of optofluidic ring resonator lasers with liquid waveguides

Jonathan D. Suter,<sup>1,2</sup> Wonsuk Lee,<sup>1</sup> Daniel J. Howard,<sup>2</sup> Eric Hoppmann,<sup>3</sup> Ian M. White,<sup>3</sup> and Xudong Fan<sup>1,\*</sup>

<sup>1</sup>Department of Biomedical Engineering, University of Michigan, 1101 Beal Avenue, Ann Arbor, Michigan 48109, USA

<sup>2</sup>Department of Biological Engineering, Bond Life Sciences Center, University of Missouri, Columbia, Missouri 65211, USA

<sup>3</sup>Fischell Department of Bioengineering, 2241 Kim Engineering Building, College Park, Maryland 20742, USA

\*Corresponding author: xsfan@umich.edu

Received June 24, 2010; revised August 2, 2010; accepted August 2, 2010;

posted August 13, 2010 (Doc. ID 130664); published August 27, 2010

Optofluidic lasers are of particular interest for lab-on-a-chip-type devices, with broad spectral tunability, convenient microfluidic integration, and a small footprint. Optofluidic ring resonator (OFRR) lasers are advantageous in terms of size but typically generate nondirectional emission that is of minimal practical use. We introduce two unique geometries for soft-lithography-based OFRR lasers—side-coupled rings and spiral rings—both of which can be produced in polydimethyl siloxane substrates with contact molding. These rings utilize evanescent and direct butt-coupling, respectively, to effectively couple the OFRR laser emission into microfluidic channels. A laser threshold of a few to tens of  $\mu\text{J}/\text{mm}^2$  is achieved. © 2010 Optical Society of America

OCIS codes: 230.5750, 170.4520, 140.2050, 140.3325.

Optofluidic or microfluidic dye lasers have recently emerged as a promising lab-on-a-chip technology because of their dynamically tunable emission spectrum, potential of integration with microfluidics, and compact size [1]. Some demonstrated designs of optofluidic dye laser cavities include distributed feedback gratings [2,3], circular Bragg gratings [4], and Fabry–Perot cavities [5,6]. Optical ring resonators are another very attractive design, utilizing circumferential resonances called whispering gallery modes (WGMs) to provide the optical feedback for lasing. Some advantages of ring resonators over linear cavities include small size and high  $Q$  factor, creating low lasing thresholds [7–9].

Optofluidic ring resonator (OFRR) dye lasers require solutions for directional outcoupling of their laser emission; otherwise it is scattered omnidirectionally, limiting its usefulness. Recently, successful coupling of OFRR laser emission has been demonstrated via a microfiber-knot-based ring resonator [10] and through evanescent coupling using a tapered optical fiber [8,9]. While those demonstrations show coupling of OFRR laser emission into solid waveguides, OFRR laser coupling into a liquid channel remains largely unexplored. Direct coupling into a liquid channel allows for integration of OFRR lasers with optofluidic components, control of the OFRR/waveguide coupling via refractive index (RI) tuning, and direct delivery of the laser signal to desired microfluidic locations.

Recently, Li *et al.* demonstrated such coupling between a liquid ring resonator and a liquid-filled waveguide [11]. This microfluidic ring resonator structure has a fluidic connection with the waveguide such that dye fills both of them. However, this design may be problematic, because dye in the waveguide will reabsorb the lasing signal, potentially contaminate optofluidic components, damage biological samples, and generate unwanted fluorescence background signal.

In this Letter, we propose and demonstrate two schemes to couple the OFRR dye laser emission into a physically separated liquid waveguide channel. In the first scheme [Figs. 1(a) and 1(b)], the liquid waveguide

is separated from the OFRR by a solid-state gap. Side coupling is achieved through the evanescent interaction between the WGM in the OFRR and the mode in the liquid waveguide [12]. In the second scheme [Fig. 1(c)], we employ a spiral ring resonator [13,14], which can be described by  $r(\theta) = r_0(1 + \varepsilon\theta/2\pi)$ , where  $r$  and  $\theta$  are the spiral radius and the angle, respectively.  $r_0$  is the initial spiral radius and  $\varepsilon$  is the deformation parameter. The spiral ring resonator's unidirectional emission into a separate liquid waveguide uses direct, nonevanescent butt-coupling. Each scheme resolves the laser emission outcoupling problem, thus enhancing the OFRR laser's versatility.

Each ring is fabricated in polydimethyl siloxane (PDMS). The side-coupled rings have an outer diameter (OD) of approximately 400  $\mu\text{m}$ , an inner diameter (ID) of 240  $\mu\text{m}$ , and a depth of 10  $\mu\text{m}$ . The liquid channel has a width of 40  $\mu\text{m}$  and a depth of 10  $\mu\text{m}$ . The waveguide is separated from the ring by a 2  $\mu\text{m}$  PDMS gap [Fig. 1(a)]. The spiral ring resonator has an initial OD of 400  $\mu\text{m}$  and ID of 240  $\mu\text{m}$ .  $\varepsilon$  is chosen to be 0.1, so the notch width is 20  $\mu\text{m}$ . The notch is separated from the liquid-filled waveguide by about 40  $\mu\text{m}$ . In both structures, the 240  $\mu\text{m}$  diameter central PDMS disk does not interact with the WGMs contributing to the lasing signal, only limiting unwanted fluorescence background.

A silicon wafer is fabricated using standard reactive ion etching procedures. The etched wafer is vacuum coated with trichlorosilane as a release layer and then coated with a 4 mm layer of mixed and degassed PDMS, and heated at 75 °C for 30 min before being released.

The experimental setup [Fig. 2(a)] uses a microsyringe to introduce R6G (or LDS 722) dissolved in tetraethylene glycol (TEG) into the OFRR while the waveguide is filled with TEG alone. After plasma treatment, the solvent quickly wicks to fill the entire structure. TEG has a RI of approximately 1.46, slightly higher than PDMS ( $\sim 1.42$ ), so it is able to guide light. The OFRR laser is pumped by a 5 ns pulsed optical oscillator at 532 nm parametric with a spot size of approximately 10  $\text{mm}^2$ . The emission is collected by an optical fiber (600  $\mu\text{m}$  in core diameter)

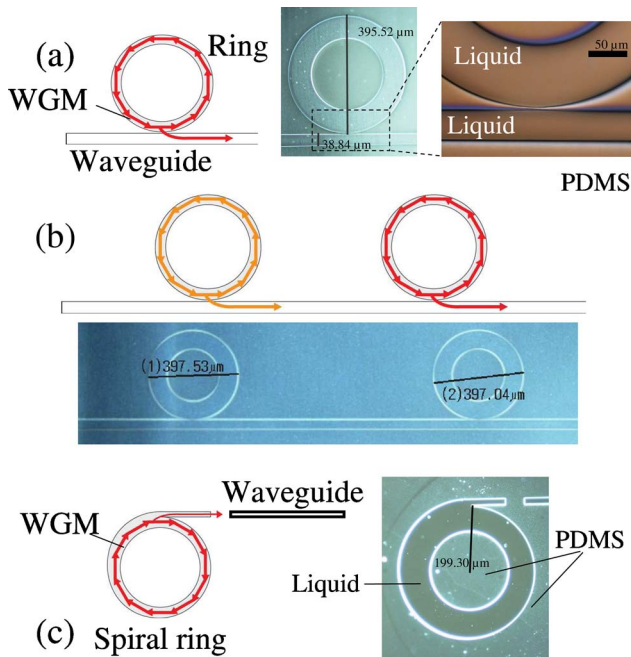


Fig. 1. (Color online) (a) Schematic and corresponding image of a single side-coupled OFRR laser, (b) two side-coupled OFRR lasers, and (c) a spiral OFRR. All the ring resonators are filled with dye in TEG, whereas the waveguides are filled only with TEG. The magnified region in (a) shows the  $2 \mu\text{m}$  PDMS gap separating the OFRR and the waveguide.

at the terminal of the liquid waveguide [Fig. 2(a)] and sent to a spectrometer (Horiba iHR550,  $\sim 0.1 \text{ nm}$  spectral resolution) for post-analysis. The  $Q$  factors of the side-coupled ring resonator and the spiral resonator are approximately 5000 (limited by the spectrometer resolution) and 750, respectively.

We first investigate the side-coupled OFRR filled with 2 mM R6G. While pumping the OFRR, strong lasing output can be observed from the end of the waveguide and some scattered light can be observed from the ring itself, generated by both fluorescence and laser emission [Fig. 2(a)]. The very dim waveguide body (contrasted with the bright terminus) suggests that (1) the ring and the waveguide are unconnected and (2) the light is directionally coupled into the waveguide. Note that, while the side-coupling is bidirectional, only one end of the waveguide is imaged in Fig. 2(a).

To further confirm this directional coupling, a fiber is placed very close to the waveguide output and moved by small increments [Fig. 2(b)]. As plotted in Fig. 2(c), groups of clustered laser peaks, resulting from the multi-transverse mode nature of the ring resonator [10,15], emerge when the fiber centers on the waveguide. When the fiber is slightly displaced from the waveguide, only featureless background is observed. Note that, although in a typical side-coupled ring resonator design, the air gap between ring and waveguide is required to be much narrower than  $1 \mu\text{m}$ , efficient coupling is possible across a larger gap ( $2 \mu\text{m}$ ) when the ring and the waveguide are surrounded by PDMS because of the large extension of the electric field in the evanescent fields resulting from the low RI contrast [16].

The side-coupling design allows for fabrication of multiple OFRRs on a single waveguide channel so that multi-

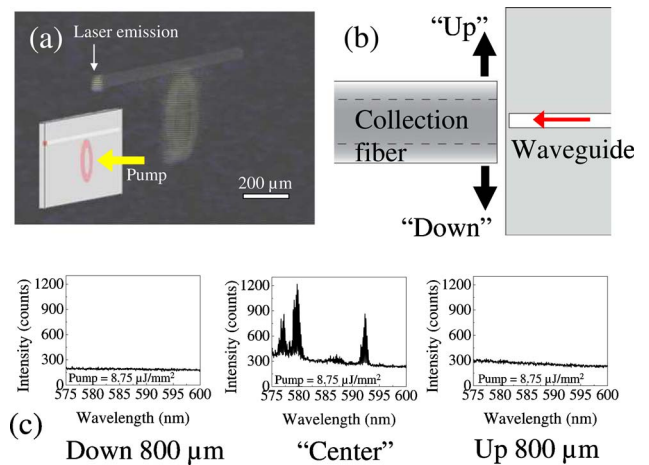


Fig. 2. (Color online) Demonstration of outcoupling of the OFRR laser emission into a TEG-filled liquid waveguide. (a) Photograph of the OFRR and the waveguide during laser operation. Inset illustrates the experimental setup. (b) Alignment schematic of a collection fiber at the end of the waveguide. (c) Spectra with the collection fiber in and out of alignment when pumping energy is  $8.75 \mu\text{J}/\text{mm}^2$ .

ple color emission into a single waveguide is possible. Figure 3 demonstrates this effect using 2 mM R6G for one ring [Fig. 3(a)] and 2 mM LDS 722 for the adjacent one [Fig. 3(b)]. The lasing threshold is approximately  $3.7 \mu\text{J}/\text{mm}^2$  [Fig. 3(c)] and  $4 \mu\text{J}/\text{mm}^2$  [Fig. 3(d)] for R6G and LDS 722, respectively, on par with past demonstrations [2,17,18]. We estimate the laser output intensity to be  $0.1 \text{ nW}$  from the side-coupled ring with LDS 722 when pumped at  $6.8 \mu\text{J}/\text{mm}^2$ . The coupling efficiency between the ring and waveguide is approximately 3%, significantly lower than that for glass-capillary-based lasers ( $\sim 50\%$ ) [17] due to much higher losses (or lower  $Q$  factors) in these rings fabricated by the contact molding method.

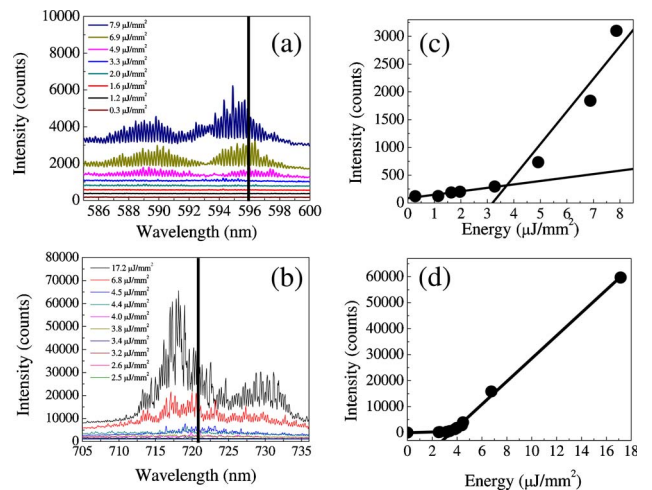


Fig. 3. (Color online) Concomitant lasing emission spectra from the waveguide for the dual-ring configuration with (a) 2 mM R6G and (b) 2 mM LDS 722 in each ring. Both rings are simultaneously pumped. The spectra recorded are vertically shifted for clarity. (c) and (d) are the corresponding laser emission intensities [at the wavelength marked by the black vertical line in (a) and (b)] as a function of the pump energy density. The lasing thresholds are 3.7 and  $4 \mu\text{J}/\text{mm}^2$  for R6G and LDS 722, respectively.

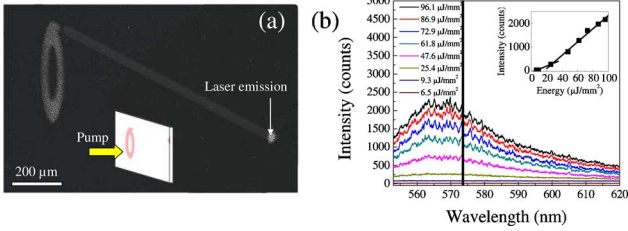


Fig. 4. (Color online) (a) Photograph of the spiral OFRR and the waveguide during laser operation. Inset shows the PDMS slab and pump beam orientation. (b) The corresponding laser emission spectra from the waveguide. Curves are vertically shifted for clarity. Inset is the corresponding laser emission intensity (at the wavelength marked by the black vertical line) as a function of the pump energy density. The estimated lasing threshold is  $26 \mu\text{J}/\text{mm}^2$ .

Figure 4 demonstrates unidirectional emission from a spiral OFRR notch defect [13,14], in contrast to bidirectional emission in the side-coupling design [Fig. 1(a)]. There are no stringent requirements on the size of the gap between the spiral ring and the waveguide, making the fabrication much easier. Figure 4(a) shows that strong laser emission can be observed at the end of the waveguide during pumping, while the waveguide itself is nearly invisible, suggesting that the laser is coupled into and guided by the waveguide. Figure 4(b) shows the actual lasing spectrum obtained from the end of this waveguide. The lasing threshold is approximately  $26 \mu\text{J}/\text{mm}^2$ , higher than that for the side-coupled ring resonator, due to the lower  $Q$  factor of the spiral. The lasing peaks are superimposed on a broad fluorescence background that likely comes from the fluorescence in the notch portion of the spiral. In contrast, the evanescent coupling scheme in Figs. 2 and 3 significantly suppresses the OFRR fluorescence background, as only the lasing modes can be coupled into and subsequently guided by the liquid waveguide.

In summary, in this Letter we have presented two schemes for outcoupling the OFRR laser emission into a liquid channel using evanescent side-coupling and direct butt-coupling methods. These configurations enable physical separation of the fluids in the laser cavities and waveguides, allowing for independent control of each optofluidic component. The laser threshold is on the order of a few  $\mu\text{J}/\text{mm}^2$  for the side-coupled ring resonator and approximately  $26 \mu\text{J}/\text{mm}^2$  for the spiral ring resonator.

Future work will involve generating a single-mode OFRR, improving fabrication to increase the  $Q$  factor,

and coating the liquid channel with extremely low-index materials, such as Teflon [19] and nanoporous silicates [20], so that biological buffer (containing mainly water) can be used to guide light in the liquid channel.

This work is supported by National Science Foundation (NSF) (ECCS-0853399) and the Wallace H. Coulter Foundation Early Career Award. J. D. S. is supported by the National Institutes of Health (NIH) Biodetectives Training Grant.

## References

1. C. Monat, P. Domachuk, and B. J. Eggleton, *Nat. Photon.* **1**, 106 (2007).
2. Z. Y. Li, Z. Y. Zhang, T. Emery, A. Scherer, and D. Psaltis, *Opt. Express* **14**, 696 (2006).
3. S. Balslev and A. Kristensen, *Opt. Express* **13**, 344 (2005).
4. Y. Chen, Z. Li, Z. Zhang, D. Psaltis, and A. Scherer, *Appl. Phys. Lett.* **91**, 051109 (2007).
5. B. Helbo, A. Kristensen, and A. Menon, *J. Micromech. Microeng.* **13**, 307 (2003).
6. D. V. Vezenov, B. T. Mayers, R. S. Conroy, G. M. Whitesides, P. T. Snee, Y. Chan, D. G. Nocera, and M. G. Bawendi, *J. Am. Chem. Soc.* **127**, 8952 (2005).
7. H.-M. Tzeng, K. F. Wall, M. B. Long, and R. K. Chang, *Opt. Lett.* **9**, 499 (1984).
8. S. I. Shopova, H. Zhu, and X. Fan, *Appl. Phys. Lett.* **90**, 221101 (2007).
9. S. Lacey, I. M. White, Y. Sun, S. I. Shopova, J. M. Cupps, P. Zhang, and X. Fan, *Opt. Express* **15**, 15523 (2007).
10. X. Jiang, Q. Song, L. Xu, J. Fu, and L. Tong, *Appl. Phys. Lett.* **90**, 233501 (2007).
11. Z. Li, Z. Zhang, A. Scherer, and D. Psaltis, in *IEEE/LEOS Summer Topical Meeting* (IEEE, 2007), pp. 70–71.
12. J. D. Suter, D. J. Howard, E. Hoppmann, I. M. White, and X. Fan, *Proc. SPIE* **7579**, 75790Y (2010).
13. X. Wu, H. Li, L. Liu, and L. Xu, *Appl. Phys. Lett.* **93**, 081105 (2008).
14. A. W. Poon, X. Luo, H. Chen, G. E. Fernandes, and R. K. Chang, *Opt. Photonics News* **19**, 36 (2008).
15. S. V. Frolov, M. Shkunov, Z. V. Vardeny, and K. Yoshino, *Phys. Rev. B* **56**, R4363 (1997).
16. P. Polynkin, A. Polynkin, N. Peyghambarian, and M. Mansuripur, *Opt. Lett.* **30**, 1273 (2005).
17. J. D. Suter, Y. Sun, D. J. Howard, J. A. Viator, and X. Fan, *Opt. Express* **16**, 10248 (2008).
18. J. C. Galas, J. Torres, M. Belotti, Q. Kou, and Y. Chen, *Appl. Phys. Lett.* **86**, 264101 (2005).
19. R. Manor, A. Datta, I. Ahmad, M. Holtz, S. Gangopadhyay, and T. Dallas, *IEEE Sens. J.* **3**, 687 (2003).
20. J. Memisevic, V. Korampally, S. Gangopadhyay, and S. A. Grant, *Sens. Actuators B* **141**, 227 (2009).